Academic Journal of Science and Technology
ISSN: 2771-3032 | Vol. 14, No. 3, 2025

Push Force Analysis Optimization Based on Differential Evolution Method

Xudong Zhang*, You Yang, Xiang Zhang, Kangyou Dou, Yaru Dang, Pengfei Zhang

School of Mechanical Engineering, Xi'an shiyou University, Xi'an 710065, China
*Corresponding author: Xudong Zhang (Email: 18329497638@163.com)

Abstract: This paper conducts an in-depth structural optimization study on the actuator of the push-off type rotary steering drilling tool based on the differential evolution method. By using the "force synthesis model" and through systematic sensitivity analysis and intelligent optimization algorithms, the influence laws of key operating parameters on the push-off force are revealed, and the design scheme of the actuator is successfully optimized. The research results show that: In the stable stationary state: when the high-pressure hole angle is set to 90°, the turntable speed is 200 r/min, and the oscillation speed is 0 r/min, the push-off force can be stably maintained at 13.5 KN, meeting the design requirements; In the clockwise oscillation state: when the high-pressure hole angle is 90°, the turntable speed is 200 r/min, and the oscillation speed is 200 r/min, the push-off force also reaches the target value of 13.5 KN; In the counterclockwise oscillation state: under the condition that the high-pressure hole angle is 90°, the turntable speed is 200 r/min, and the oscillation speed is 100 r/min, the push-off force can still be stably maintained at 13.5 KN. The final optimization scheme is confirmed as follows: the high-pressure hole angle is preferably set to 90°, the turntable speed is fixed at 200 r/min, and the oscillation speed of the control axis can be flexibly adjusted according to the actual working conditions.

Keywords: Rotary steering drilling tool; Thrust force; Equivalent force synthesis model; Differential evolution method.

1. Introduction

Against the backdrop of the ever-rising global energy demand, oil and gas resources, as the main energy pillars, are gradually being explored and developed in complex areas such as deep sea, deep layers, and unconventional reservoirs. This trend poses unprecedented challenges to drilling technology, with efficient drilling and precise wellbore trajectory control being the key to the economic and effective development of complex oil and gas reservoirs.

The control methods of traditional rotary steerable drilling tools have played a significant role in past oil and gas development. However, in the face of today's complex and variable geological conditions and increasingly strict drilling requirements, their limitations have become increasingly prominent. Take the push-the-bit rotary steerable system as an example. The optimization and control of lateral push force is the key mechanism for adjusting the wellbore trajectory. However, existing technologies have obvious deficiencies in the precise control and optimization of lateral push force. On the one hand, it is difficult to adjust the push force in real time according to different formation characteristics, resulting in insufficient push force in hard formations and ineffective steering, and excessive push force in soft formations causing wellbore wall damage. On the other hand, uneven distribution of push force can easily lead to bit wear and drill string vibration, reducing drilling efficiency and tool life, and affecting the control accuracy of the wellbore trajectory.

Therefore, the optimization analysis of the lateral push force of rotary steerable drilling tools has become a core issue that needs to be urgently addressed in the current drilling engineering field. The new steering control method aims to break through the bottlenecks of traditional technology and adjust and optimize the parameters of the hydraulic control system of the lateral push force by combining optimization algorithms. By precisely controlling the lateral push force, the drill bit can more accurately follow the predetermined trajectory, effectively reducing the frictional resistance between the drill string and the wellbore wall, increasing the mechanical drilling rate, and simultaneously reducing the probability of complex situations such as wellbore instability and keyhole formation, thereby significantly improving drilling efficiency and wellbore quality.

This paper focuses on the optimization analysis of the lateral push force in the new steering control method of rotary steerable drilling tools, deeply explores the various factors affecting its strength and conducts optimization analysis, providing useful references and lessons for promoting the innovative development of rotary steerable drilling technology.

1.1. Composition of the Hydraulic Control System

The hydraulic control system is a key component of the anti-deviation actuator, mainly consisting of the control shaft, upper disk valve, and lower disk valve, as shown in Figure 1 below.

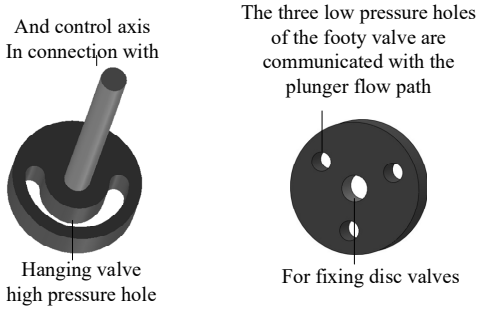

Figure 1. Composition of the Hydraulic Control System

Their function is to execute the control instructions of the

rotary steering drilling control system, control the distribution of drilling fluid flow, and ensure that the actuator can generate a certain direction and magnitude of wing rib push force. The magnitude and direction of the resultant force are mainly controlled by the control shaft. The upper disk valve is connected to the control shaft of the drilling tool's stable control platform, and the control shaft controls the upper disk valve. The upper disk valve is equipped with a high-pressure hole, which is in an arc shape. The purpose is to ensure that the high-pressure drilling fluid has a certain high-pressure action time to guarantee the control effect of the lateral force of the drill bit, and at the same time ensure that at least one wing rib is always in contact with the wellbore wall, reducing the impact of the push force on the drilling tool. The lower disk valve is installed inside the actuator body and rotates together with the actuator body and the drill string. The lower disk valve has three evenly distributed flow holes along the circumference, which are respectively connected to the flow channels of the three push mechanisms. When the high-pressure hole of the upper disk valve is connected to the flow hole of the lower disk valve, the drilling fluid flows through the upper and lower disk valves to the push block, and then through the pressure relief hole on the push block, flows into the annulus between the drilling tool and the outer wall, thereby generating a certain pressure drop. Under the action of the pressure drop, the push block moves upward and generates a certain thrust, pushing the push wing ribs to extend outward and push against the wellbore wall, generating a certain magnitude and direction of push force.

2. The Principle of the "Equivalent Force Synthesis Model" Section Headings

The control method adopted in this paper, the "equal force synthesis model" of guidance force, is consistent with the principle of adjusting the guidance force of rolling-type missiles. It adjusts the magnitude of the guidance force by adjusting the swing amplitude of the control surfaces, and can achieve continuous adjustment of the guidance force. As the swing amplitude of the control surfaces increases, the guidance force gradually decreases, but when the swing amplitude is small, the decrease in magnitude is very small.

When the maximum guidance force is required, the control axis stabilizes in a fixed direction. At this time, the direction of the high-pressure hole on the control valve remains constant, and the resultant force direction of the action force of the guidance mechanism is opposite to that direction. During the guidance process, sometimes it is not necessary to work in the maximum guidance force mode. In such cases, the control axis can swing around a certain equilibrium direction. The magnitude of the resultant force is determined by the swing amplitude, and the direction of the resultant force is the equilibrium direction. When the swing amplitude reaches a certain degree, the guidance mechanism will lose its guidance ability, and the entire drill string becomes a tool without guidance ability and is in a "neutral" working state. For the convenience of description, the resultant force direction of the guidance force is referred to as the "tool face direction" hereinafter. The plane containing the control axis and the high-pressure valve hole at any instant is called the control surface. Figure 2 shows the lateral force distribution of the guidance drill string assembly in the general guidance state. It can be seen that the equilibrium swing direction of the control axis is the direction AD, that is, the direction of the vector Fk in the figure, which represents the tool face direction[12].

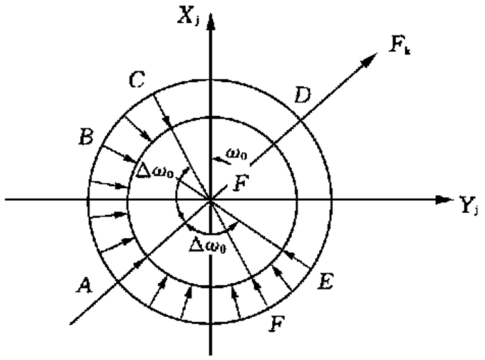

Figure 2. Vector of the resultant force of the axial force

The "equivalent force synthesis model" regarding the lateral pushing and backing force is as follows:

$$F_K = F_O \frac{\sin \Delta\omega_0}{\Delta\omega_0} \left(0 \le \Delta\omega \le \pi\right) \tag{1}$$

In the formula, F_0 represents the force exerted by the palm on the wellbore wall at a certain instant; ω_0 is the tool face angle under the general directional condition; $\Delta\omega_0$ is the amplitude of the control axis swing.

The value of the average resultant force F_k, F_k, depends on the value of $\Delta\omega_0$. As $\Delta\omega_0$ increases, the value of the average resultant force F_k gradually decreases from F_0 to zero. The adjustment of the guiding resultant force can be achieved by controlling the swing of the control surface. When the swing amplitude $\Delta\omega_0$ is larger (up to π), the resultant force becomes smaller.

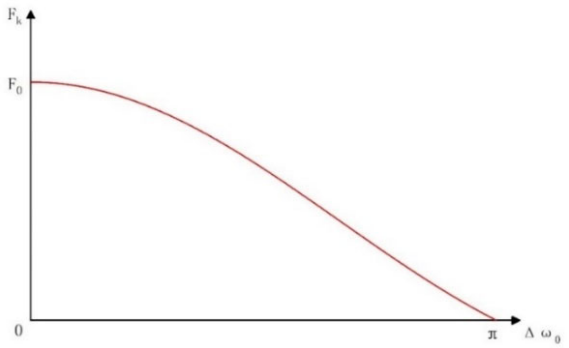

Figure 3. Curve of the guiding force varying with $\Delta\omega_0$

According to Figure 3, the working state and the magnitude of the guiding force of the guiding mechanism can be summarized as follows:

When $\Delta\omega_0 = 0$,at this time it is in the state with the maximum guiding force, and the tool face direction is determined by ω_0;

$$F_k = F_0 \tag{2}$$

At that time, when $\Delta\omega_0 = \pi$, the system was in a "neutral" working state.

$$F_k = 0 \tag{3}$$

At this time, when $0<\Delta\omega_0<\pi = \pi$the tool face direction is determined by ω0 and the tool is in the normal working state.

$$F_k = F_0 \frac{sin\Delta\omega_0}{\Delta\omega_0} \tag{4}$$

According to the formula for the rotational speed of the turntable, we can obtain:

Table 1. Working Status of Control Surface under General Operating Conditions

Working status	The control surface remains stable and unchanged.	The control surface makes counter clockwise stable oscillation.	The control surface makes a clockwise stable oscillation.
Durationof high-pressure action	$t_0 = \frac{\gamma}{3n_z}$	$t_0 = \frac{\gamma}{3(n_z - n_b)}$	$t_0 = \frac{\gamma}{3(n_z + n_b)}$

In the formula, the rotational speed of the turntable is n_z, and the swing speed of the control surface is n_b, r/min; the central angle corresponding to the high-pressure valve hole is γ, (°).

During the high-pressure action time, the effect of the telescopic block on the telescopic wing rib can be regarded as an equivalent force synthesis model within the time of t0. The general relationship between the angular velocity and the rotational speed is:

$$\omega = 2\pi n \tag{5}$$

Since within a certain amplitude range, the oscillation speed of the control surface gradually increases from zero until it reaches the maximum value and then gradually decreases back to zero, its equivalent oscillation amplitude can be expressed as:

$$\Delta\omega_0 = \frac{n_b \pi}{120} t_0 \tag{6}$$

Then the resultant force of the single telescopic block acting on the telescopic wing ribs can be expressed as:

$$F_{k0} = \frac{120F_0}{n_b t_0 \pi} \sin\left[\frac{n_b \pi}{120} t_0\right] \tag{7}$$

3. Sensitivity Analysis

3.1. Influence of Swing Speed on Pushing Force

Assuming that the rotational speed of the turntable is n_z = 60 r/min and the angle of the high-pressure hole γ = 120°, the variation pattern of the pushing force with the swing speed is as shown in Figure 4. From the figure, it can be seen that the pushing force will show three different trends under three states. When the control axis swings clockwise, the pushing force gradually decreases steadily and the variation range is small. When the control axis swings counterclockwise, the pushing force drops significantly before reaching 50 r/min, fluctuates at 0 r/min, and gradually increases to F_{k0} after the swing speed reaches 80 r/min. When the control axis remains stable, the pushing force does not change.

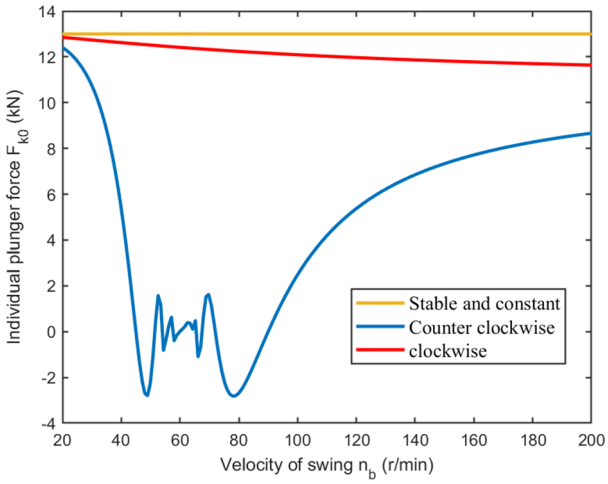

Figure 4. The variation of the pushing force with the swing speed

3.2. Influence of Spindle Speed on Pushing and Tilting Force

Assuming that the oscillation speed n_b = 100 r/min and the angle γ of the high-pressure hole is 120°, the variation law of pushing and tilting force with spindle speed is shown in Figure 5. From the figure, it can be seen that the spindle speed in different states will also present three different trends. When the control shaft swings clockwise, the pushing and tilting force gradually increases stably and the variation range is small. When the control shaft swings counterclockwise, the pushing and tilting force drops significantly before reaching 68 r/min, fluctuates between 68 and 120 r/min, and gradually increases to F_{k0} after the spindle speed reaches 122 r/min. When the control shaft remains stable, the pushing and tilting force does not change.

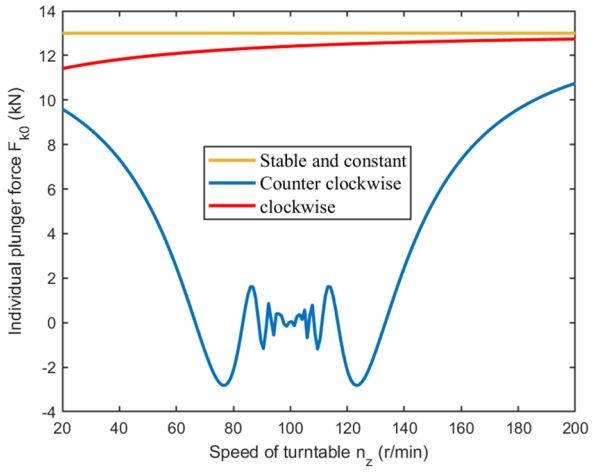

Figure 5. Variation of the pushing force with the speed of the turntable

3.3. Influence of the Angle of High-pressure Hole on the Pushing Force

When the oscillation speed taken is too high, the pushing force gradually changes in a zigzag manner as the angle of the high-pressure hole increases, and the greater the oscillation speed, the steeper the zigzagging becomes as shown in Figure 6 below.

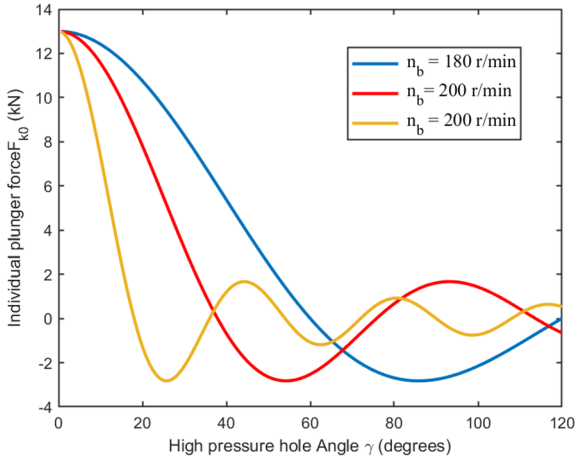

Figure 6. The variation pattern of the pushing and relying force with the angle of the high-pressure hole when the oscillation speed is high.

Therefore, when the oscillation speed n_b = 100 r/min and the rotation speed of the turntable n_z = 60 r/min are set, the variation law of the push-off force with the angle of the high-pressure hole is as shown in Figure 7. From the figure, it can be concluded that the push-off force gradually decreases as the angle of the high-pressure hole increases. Among them, the deceleration speed in the counterclockwise direction is the greatest, and the deceleration speed in the clockwise direction is not obvious.

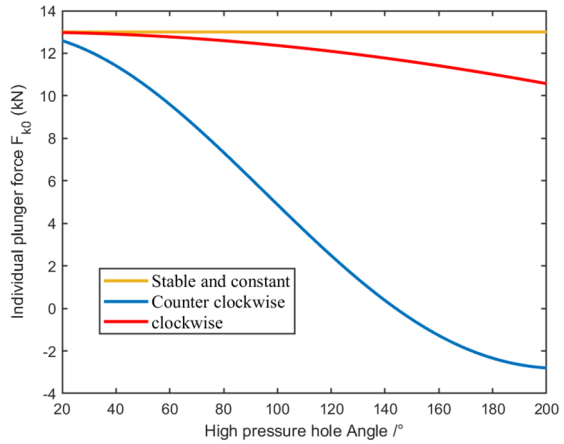

Figure 7. Variation of the pushing force with the Angle of the high-pressure hole

3.4. Influence of multiple factors

Set the oscillation speed to 50 r/min and 100 r/min respectively. The variation law of the resultant force F_{k0} exerted by a single telescopic block on the wellbore wall with the oscillation speed: When the control surface remains stable and does not move, the oscillation speed is 0, and theoretically the magnitude of the resultant force is equal to the force exerted by the plunger on the wellbore wall. When the control surface rotates counterclockwise and clockwise, the relationship between the rotational speed of the turntable, the angle of the high-pressure hole and the guiding resultant force.

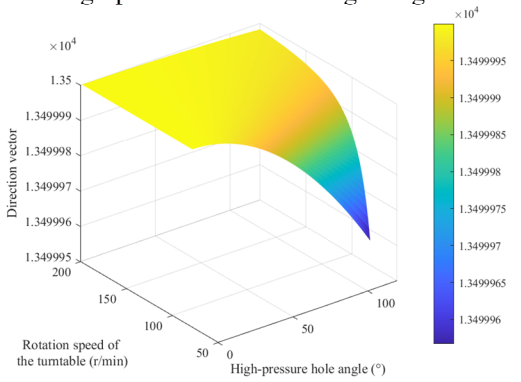

(a) The control surface is counterclockwise (50r/min)

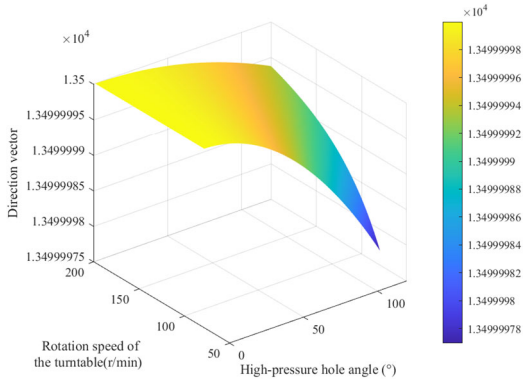

(b) The control surface is clockwise (50r/min)

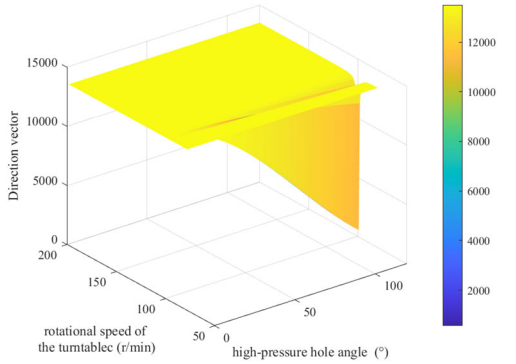

(c) The control surface is clockwise (100r/min)

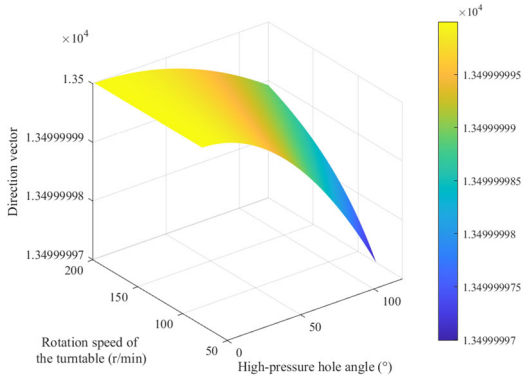

(d) The control surface is clockwise (100r/min)

Figure 8. The relationship between the rotary speed of the turntable and the Angle of the high-pressure hole and the resultant force of the guide under different states of the control surface

From the above Figure 8, it can be concluded that when the oscillation speed is relatively low, regardless of the state of the control surface, as the angle of the high-pressure hole

increases, the guiding force shows a decreasing trend, and the increasing trend becomes increasingly acute; as the rotational speed of the turntable increases, the guiding force shows a decreasing trend, and the decreasing trend remains almost unchanged. However, when the oscillation speed is relatively high, the trend of the guiding force caused by the clockwise rotation of the control surface is not significantly different from that when the oscillation speed is relatively low, but the guiding force caused by the counterclockwise rotation of the control surface will show obvious fluctuations.

4. Differential Evolution Algorithm and Optimization Results

4.1. Operation Steps

Differential Evolution Algorithm (DE) is also an optimization algorithm based on modern intelligent theory. It guides the direction of optimization search through the group intelligence generated by the mutual cooperation and competition among individuals within the group. The specific operation steps are as follows:

(1) Mutation

When the population evolves to the Gth generation, the mutation operation is performed on the parent individual Xi,G to obtain the mutated individual, that is:

$$V_{i,\ G+1} = X_{r1,\ G} + F \cdot \left(X_{r2,\ G} - X_{r3,\ G} \right) \quad (8)$$

In the formula, the subscripts r1, r2, r3 are randomly selected distinct integers different from i within the range of 1 and NP (population size). X_{r1},G is called the base vector, (X_{r2},G - X_{r3},G) is called the difference vector, and F is the scaling factor. If the parameters of the mutated individual exceed the boundaries, the value of that parameter will be replaced by the boundary value.

(2) Cross-over

The experimental individuals generated through cross-over operation are:

$$U_{i,\ G+1} = \left[u_{1,\ i,\ G+1}, \cdots,\ u_{j,\ i,\ G+1}, \cdots,\ u_{D,\ i,\ G+1} \right] (9)$$

Among them,

$$U_{j,\ i,\ G+1} = \begin{cases} v_{j,\ i,\ G+1}, if \quad r_j[0,1) \le CR \\ or \quad j = r(i) \\ x_{j,i,G}, otherwise \end{cases} \quad (10)$$

In the formula, rj[0,1) represents the random number of the jth calculation, and CR is the crossover rate. r(i) is an integer randomly selected between 1 and D, which enables Ui,G+1 to obtain at least one variable from Vi,G+1.

(3) Selection

For the minimization problem, the individuals with smaller objective function values in the trial individual Ui,G + 1 and the parent individual Xi,G are selected to enter the next generation population, that is:

$$X_{i,\ G+1} = \begin{cases} U_{i,\ G+1}, if \quad F\left(U_{i,G+1}\right) < F\left(X_{i,G}\right) \\ X_{i,G},\ \text{otherwise} \end{cases} \quad (11)$$

In the formula, F(X) represents the objective function.

The main control parameters in the algorithm are population size NP, scaling factor F, and crossover rate CR. Usually, these parameters remain unchanged during the evolution.

4.2. Optimization Analysis Results

As shown in Figure 6, as the angle of the high-pressure hole increases, the pushing force gradually decreases. Therefore, the angle of the high-pressure hole should not be too large. However, since the angle of the high-pressure hole should ensure a certain duration of high-pressure action, it should not be too small. The final determined parameter range is shown in Table 2. Other parameter settings of the differential evolution algorithm are as follows: population size NP = 100; scaling factor F = 0.5; crossover factor CR = 0.7; maximum number of iterations G_MAX = 100; parameter dimension D = 3.

Table 2. Parameter Range

Parameter	High-pressure hole angle /°	Rotation speed of the turntable r/min	Swing speed r/min
Range	90~120	60~200	40~200

From the previous text, it can be known that the working state should be discussed in three states. The optimization results are obtained through differential evolution method analysis, as shown in Table 3.

Table 3. Optimization Results

Status	High-pressure hole angle /°	Rotation speed of the turntable r/min	Swing speed r/min
Remains stable and unchanged.	90	200	0
Makes counter clockwise stable oscillation.	90	200	200
Makes clockwise stable oscillation.	90	200	100

When the control shaft is in a stable and immobile state, the angle of the high-pressure hole is set at 90°, the rotational speed of the turntable is set at 200 r/min, and the oscillation speed is set at 0 r/min. The pushing force remains unchanged at 13.5KN. When the control shaft is in a clockwise oscillation state, the angle of the high-pressure hole is set at 90°, the rotational speed of the turntable is set at 200 r/min, and the oscillation speed is set at 200 r/min, the pushing force can reach the required value of 13.5 KN. When the control shaft is in an anti-clockwise oscillation state, the angle of the high-pressure hole is set at 90°, the rotational speed of the turntable is set at 200 r/min, and the oscillation speed is set at 100 r/min, the pushing force can reach the required value of 13.5 KN. Finally, the high-pressure hole angle is determined to be 90°, the rotational speed of the turntable is set at 200 r/min, and the oscillation speed of the control shaft will be adjusted according to the actual situation.

5. Conclusion

In this study, firstly, the influence degree of each influencing factor affecting the pushing force is analyzed, and the change law of the pushing force with the swing speed, the rotating speed of the turntable and the Angle of the high-pressure hole is obtained. After comparison, it is found that the influence degree of the swing speed is large, and the influence degree of the Angle of the high-pressure hole is small. Furthermore, based on the equal force synthesis model, the differential evolution method is used to systematically optimize the key parameters that affect the lateral push force, such as the high-pressure hole Angle, the rotary speed and the swing speed. Through multiple rounds of iteration and global search, we finally determined that the high-pressure hole Angle was 90°, the rotating speed of the turntable was 200r/min, and the swing speed of the control shaft was adjusted according to the actual situation, that is, 0r/min when it was stable. When rotating clockwise, it is 100r/min. The counterclockwise is 200r/min, which not only effectively ensures the high pressure time of the high pressure hole, but also ensures that the pushing force reaches the actual working condition demand. The experimental results show that the optimized parameter combination has a significant effect on improving the overall performance of the system, which not only meets the reliability of the high-pressure hole operation, but also takes into account the stability and efficiency of the pushing force. In this study, the differential evolution method shows its advantages in dealing with complex multivariate optimization problems, and provides an effective solution for parameter optimization of similar nonlinear mechanical problems. This study provides important theoretical reference and practical guidance for parameter optimization in related fields, and has positive significance for improving the performance of engineering systems.

References

[1] Liu Xiaojun. Application research and development of rotary steering-drilling technology [J]. China Petroleum & Chemical Standards & Quality,2021,41(24):195-196.

[2] Li Wei, Mou Lei, Zhou Xiancheng et al. Research progress of rotary steerable system and its control method [J]. Coal Geology and Exploration,2023,51(10):167-179.

[3] Li Xiaojun, Wang Dezhi, Jiang Bo et al. Research on WDRSS-I rotary steering Control System and Actuator [J]. Oil Field Machinery,2014,43(09):45-48.

[4] Zhao Wenzhuang, Wei Haifang, Yang Yun. Application of CG STEER rotary steering in Changqing Shale Oil H100 Platform [J]. Drilling and Production Technology,2021,44(05):1-6.

[5] Li Junqiang, Wu Xueyao, Peng Yong et al. Mechanical model and simulation analysis of control valve of regulated rotary steering-drilling tool [J]. Natural Gas Industry,2005(06):52-55+171-172.

[6] Di Qinfeng, Zhang Xiaoke, Han Laiju, et al. The description method and variation law of the effect of the regulated rotary steering-system on the wellbore wall [J]. Acta Petrolei Sinica, 2004(04):84-86+91.

[7] Li L ,Xue Q ,Liu B , et al.The dynamics of eccentric block in a fully mechanical vertical drilling tool under the effect of torsional vibration[J].Advances in Mechanical Engineering, 2018, 10(4): 1-18.

[8] Huang L ,Xue Q ,Liu B , et al. Dynamic Reliability Analysis of Rotary Steering Drilling System [J]. Mechanical Sciences, 2019, 10(1):79-90.

[9] ZHU J ,ZOU D ,ZHANG Y , et al.Design and Experimental Study of Non-contact Power Transmission Device in Static Push-type Rotary Steering Drilling System[J].Advances in Petroleum Exploration and Development,2019,18(1):73-82.

[10] Bao H T H ,Thanh H D ,Ngoc D V , et al.Multi-objective optimal power flow of thermal-wind-solar power system using an adaptive geometry estimation based multi-objective differential evolution[J].Applied Soft Computing, 2023, 149(PA): 1568-4946.

[11] Wang R ,Xue Q ,Han L , et al.Torsional vibration analysis of push-the-bit rotary steerable drilling system[J].Meccanica: Journal of the Italian Association of Theoretical and Applied Mechanics,2014,49(7):1601-1615.

[12] Qinfeng Di, Laiju Han, Mingxin Sun. Establishment and Analysis of "Equal Force Synthesis Model" for steering Force of Regulated rotary steerable System [J]. Journal of University of Petroleum (Natural Science Edition),2004,(06):35-37.

[13] Li L ,Xue Q ,Liu B , et al.The dynamics of eccentric block in a fully mechanical vertical drilling tool under the effect of torsional vibration[J].Advances in Mechanical Engineering, 2018, 10(4): 1-18.

[14] Huang L ,Xue Q ,Liu B , et al. Dynamic Reliability Analysis of Rotary Steering Drilling System [J]. Mechanical Sciences, 2019, 10(1):79-90.

[15] Wu Ning. Short-term prediction of grape downy mildew based on grey relational analysis and optimized SVM [D]. Shanghai Ocean University,2020.

[16] Zhu Hongping, Wang Xingxing. Parameter optimization of Injection molding process based on Grey Relations-entropy weight method [J]. Engineering Plastics Application, 2024, 52(09): 79-85.

[17] Yin Xiangqin, KONG Fanyu, Miao Zeyu, et al. Process Parameter Optimization of T91 Steel Pipe Welded Joint Based on Uniform Design Method [J]. Hot Working Technology, 2018, 47(01):245-248+252.

[18] Duan Guoyong, Wang Shuhan, Li Fei. Sensitivity analysis and optimization of Anchorage parameters based on uniform design method [J]. Hydropower Energy Science, 2015, 33(02): 120-123+114.

[19] LIU Lili, LIU Yupeng, Meng Fan-Li, et al. Site Value Evaluation based on entropy weight method and Differential evolution Algorithm [J]. Telecommunication Engineering Technology and Standardization, 2012,35(09):60-66.

[20] ZHANG Tiecheng, GUO Hongping, WANG Xiaonan, et al. Comprehensive Evaluation Model of Project-based Learning Based on Entropy weight-Grey Relational Analysis Method [J]. Journal of Hubei Normal University (Natural Science Edition),2024,44(03):107-112.

[21] SUN Meiqing, Yang Jianjun, Li Qingtang, et al. Piston Structure Optimization of New Mud Pump Based on Genetic Algorithm [J]. Equipment Manufacturing Technology, 2015, (01): 35-37.

[22] Pang Haowen. Optimization of Paper Honeycomb Ultrasonic Disk Cutting Tool Parameters Based on Genetic Algorithm [D]. Dalian Jiaotong University,2018.

[23] Xu Zhijie, ZHU Qiao, XU Shunfan, et al. Research on Parameter identification algorithm of lithium battery model Based on Differential Evolution Method [J]. Electrotechnical Technique,2021,(07):35-37.